

Shape and Moment Invariants Local Descriptor for Structured Images

Anonymous Submission

Anonymous Affiliation

Abstract

Finding correspondences between two images to determine if they depict the same scene or object, is a fundamental, yet challenging task. To cope with different viewpoints and lighting conditions, usually salient regions are detected as local invariant features, encoded by descriptors such as SIFT or SURF. While using the image intensities around a single point, the centroid of the region, to compute a histogram-of-gradients type descriptor, often works well, we argue that for structured scenes it is enough to use only the binary shape of the regions. We propose a 20-dimensional Shape and Moment Invariant (SMI) descriptor and show that it outperforms the 64-dimensional SURF on classical and transformation-independent datasets in terms of precision, achieving similar or even higher accuracy, while having a better scalability.

Keywords: image matching, affine-invariant descriptor, shape invariants, moment invariants

1 Introduction

Automatically determining whether 2 images depict partially the same physical scene is a fundamental computer vision problem such as baseline stereo matching, image retrieval, etc. [Escalera et al., 2007, Matas et al., 2002]). *Detection* of local (due to partial overlap) features, followed by *matching* of their *descriptors*, is the used approach. Salient regions, corresponding to the same image patches, detected with high repeatability independently in each image are such features. Many detectors and descriptors are designed to be invariant to photometric (due to different sensors and lighting) and affine geometric transformations (due to different viewpoints). In recent years, a new approach of using large datasets of image patch correspondences is established, [Snavely et al., 2008, Zagoruyko and Komodakis, 2015]. However, when very few, even only 2 *structured* (having homogeneous regions with distinctive boundaries) images are available, e. g. in some scientific applications [Ranguelova, 2016], deep learning is not applicable.

The Maximally Stable Extremal Regions (MSER) has become the standard in the field, [Matas et al., 2002]. It is often used in combination with a histogram-of-gradients type descriptor such as Scale-invariant Feature Transform (SIFT) or Speeded-Up Robust Features (SURF), [Bay et al., 2008], computed from image intensities around the centroids of the MSER regions. We argue that using the shape and moment information of the regions encoded by a *Shape and Moment Invariants (SMI)* descriptor is beneficial, compared to image intensities around the region's centroid. Figure 1 illustrates two cases of image pairs, one depicting the same scene and the other- not, when SMI outperforms SURF applied on pre-detected MSER regions.

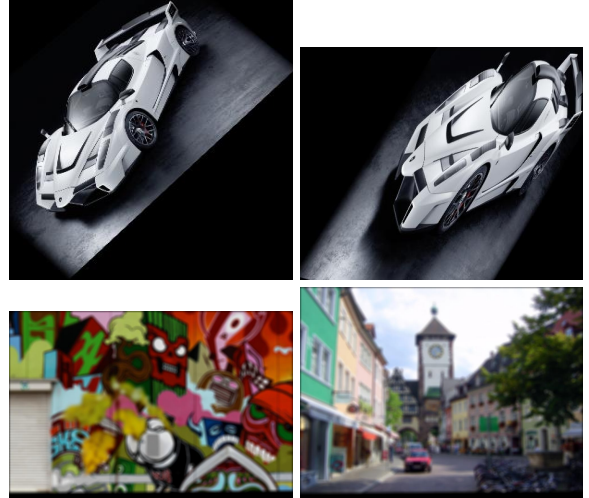


Figure 1: “Is it the same object or scene?” Matching two images under different transformation using MSER regions. *Top image pair* (scale and viewpoint): SURF descriptor yields false negative (similarity score 0.096), while SMI - true positive (0.89). *Bottom image pair* (blur): SURF gives false positive (0.27), while SMI - true negative (-0.11).

2 Related work

The literature describes large number of local detectors and descriptors, for a recent introduction and overview the reader is referred to [Hassaballah et al., 2016]. Here we mention very briefly only the closely related work.

A comparative performance evaluation of many detectors have concluded that the MSER is the best performing region detector for structured scenes, [Mikolajczyk et al., 2005]. Since, MSER has been integrated in MATLAB, OpenCV, VLFeat, etc. , making it the default baseline detector. However, despite its success, the detector has several drawbacks, which have been addressed and fixed by improved detectors, including the Data-driven Morphology Salient Regions detector (DMSR), [Ranguelova, 2016]. Here, we propose to use a Binary detector (BIN) using the first step of DMSR construction: data-driven binarization explained in [Ranguelova, 2016], with either all or only regions with large area ($A_{reg.} \geq f_A \cdot A_{Im.}$).

Another comparative performance evaluation of many region descriptors have concluded that the "region-based SIFT descriptor" is best performing again for structured images, [Mikolajczyk and Schmid, 2005]. Since, we are interested in using the binary shape shape of the detected regions, we have chosen for the moment invariant theory. Moment invariants are a group of efficient invariant object descriptors. Flusser et al. developed a coherent theory and general framework for the derivation of Affine Moment Invariants (AMIs) using graph representation [Suk and Flusser, 2004, Flusser et al., 2009].

Research has been performed not only to determine the best region detector and descriptor, but also the best combination detector - descriptor. For example, the conclusion of the experiments in [Dahl et al., 2011] is that the best combination is DOG or MSER detector and SIFT (SURF was not included in the experiments) or DAISY descriptors. SURF has been introduced as an improvement over SIFT and since has become a standard descriptor in many computer vision software libraries, making it the default baseline descriptor, [Bay et al., 2008]. Hence, we have chosen MSER + SURF as the baseline detector + descriptor combination.

3 Image matching with Shape and Moment Invariant descriptor

We propose a set of several Shape and Moment Invariants (SMI) derived from the binary shapes of the detected regions as a region descriptor. SMI descriptor contains *shape invariants* and *moment invariants*.

Shape invariants A binary shape of a region R_i can be described by a set of simple properties of the original shape or the equivalent (up to the second order moments) ellipse E_i . These are: the region's area a_i , the area of the region's convex hull a_i^c , the length of the major and minor axes of E_i , μ_i and ν_i and the distance between the foci of the ellipse ϕ_i . From these basic properties, a set of shape affine invariants are defined in Table 1.

Invariant	Definition	Description
Relative Area	$\tilde{a}_i = a_i / A$	region's area normalized by the image area A
Ratio Axes Lengths	$r_i = \nu_i / \mu_i$	ratio between E_i minor and major axes lengths
Eccentricity	$e_i = \phi_i / \mu_i$	$e_i \in [0, 1]$ (0 is a circle, 1 is a line segment.)
Solidity	$s_i = a_i / a_i^c$	proportion of the convex hull pixels, that are also in the region.

Table 1: Simple shape invariants.

Affine Moment Invariants If $f(x, y)$ is a real-valued image with N points, the AMI functional is defined by

$$I(f) = \int_{-\infty}^{\infty} \prod_{k,j=1}^N C_{kj}^{n_{kj}} \cdot \prod_{l=1}^N f(x_l, y_l) dx_l dy_l, \quad (1)$$

where n_{kj} are non-negative integers, $C_{kj} = x_k y_j - x_j y_k$ is the cross-product (graph edge) of points (nodes) (x_k, y_k) and (x_j, y_j) , [Suk and Flusser, 2004]. For full details of the AMI's theory the reader is referred to [Flusser et al., 2009]. We use the set of 16 irreducible AMIs of $N = 4$ th order as implemented by the authors in an open source MATLAB software.

Hence, the final descriptor for the i -th region is a 20 element feature vector $SMI_i = \{\tilde{a}_i, r_i, e_i, s_i, m_{i1}, \dots, m_{i16}\}$.

Matching Lets $SMI1$ and $SMI2$ be $n_1 \times 20$ and $n_2 \times 20$ matrices, where each row is the SMI descriptor for the n_1 and n_2 regions detected via MSER or BIN (all/largest) detector in the pair of images $\langle I1, I2 \rangle$. We compare exhaustively $SMI1$ and $SMI2$ with Sum of square differences metric. The matching threshold for selection of the strongest matches is mt , the max ratio threshold for rejecting ambiguous matches is mr , the confidence of a match is mc and only unique matches are allowed. Then, we select the top quality matches above a cost threshold ct . From those, we estimate in it iterations the affine transformation \tilde{T} between the two sets of points-centroids of the matching regions sets as average of nr runs with allowed max point distance md . The two images are then transformed $J2 = \tilde{T}(I1)$, $J1 = \tilde{T}^{-1}(I2)$ and a correlation ($cor[X, Y] = cov[X, Y]/\sqrt{var[X]var[Y]}$) between the original and transformed images is used for confirmation of a true match. If the average correlation similarity between both images and their transformed versions ($cor[I1, J1] + cor[I2, J2])/2$ is above a similarity threshold st , we declare the image pair $\langle I1, I2 \rangle$ to be depicting (partially) the same scene.

Figure 2 illustrates the major steps of the image matching using BIN + SMI in case of viewpoint distortion. Note the better alignment in the right part of the images due to the larger number of correct matches there. The steps are the same when using MSER instead of the data-driven binarization or SURF instead of SMI descriptor.



Figure 2: Matching two images of the same scene under viewpoint transformation using BIN regions and SMI descriptor. *First column:* original images $I1, I2$; *second column:* binarization; *third column:* matched BIN regions using SMI descriptor (blend view with pseudocolours); *fourth column:* overlay of the original and transformed images $(I1, J1), (I2, J2)$

4 Performance Evaluation

We have tested the performance of the MSER and BIN (all regions and only the largest) detectors in combinations with the SURF and SMI descriptors on 2 datasets: Oxford (VGG), [Mikolajczyk et al., 2005] and OxFrei, [Ranguelova, 2016]. Each of the 4 structured image sequences of the Oxford set consists of 1 base and 5 increasingly distorted images. Each sequence can be used to test only 1 transformation T : viewpoint, scaling + rotation, decreased lighting and blur. OxFrei dataset overcomes this limitaiton: 9 structured scenes each with 21 images (original + 5 images for $4T$) using Oxford's real homographies. We compared all possible image pairs and assigned a flag *True/False* if a pair is depicting the same scene as described inSection 3. The values of parameters used in the experiments have been determined empirically: $mt = mr = 1$, $f_A = 2e - 3$ (for BIN largest), $it = 1000$, $nr = 10$, $mc = 95$, $md = 8px$, $ct = 0.025$, $st = 0.25$. Figure 1 illustrates the result for 2 pairs and Figure 3- for all pairs (a pixel represents image pair and a square block - a sequence) of the OxFrei dataset. Note the lower number of false positives and correlation similarity variance when using the SMI descriptor.

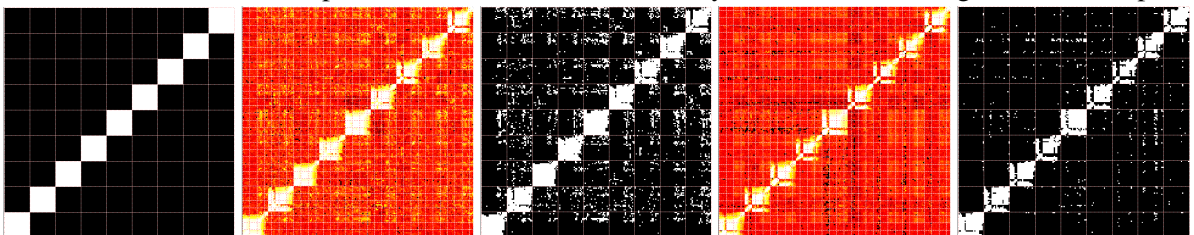


Figure 3: All pairs of the OxFrei dataset: “Is the image pair from the same scene?”. True(white)/False(black). Correlation similarity: the lighter, the higher. *First:* ground truth; *second and third:* MSER + SURF; *fourth and fifth:* MSER + SMI.

The performance results on the VGG dataset are summarized in Table 2.

Detector + descriptor	TP	TN	FP	FN	Accuracy	Precision	Recall
MSER + SURF	128	428	4	16	0.965	0.969	0.889
MSER + SMI	122	430	2	22	0.958	0.98	0.847
BIN + SURF	122	426	6	22	0.951	0.953	0.847
BIN (All) + SMI	84	432	0	60	0.89	1	0.58
BIN (Largest) + SMI	112	424	8	32	0.93	0.93	0.77

Table 2: Performance of salient region detectors and descriptors on the VGG dataset.

The performance results on the OxFrei dataset are summarized in Table 3.

Detector + descriptor	TP	TN	FP	FN	Accuracy	Precision	Recall
MSER + SURF	3309	28848	2904	660	0.90	0.53	0.83
MSER + SMI	2957	31162	590	1012	0.95	0.83	0.74
BIN + SURF	2513	28198	3554	1456	0.85	0.41	0.63
BIN (All) + SMI	1275	31298	454	2694	0.91	0.73	0.32
BIN (Largest) + SMI	2079	28474	3278	1890	0.85	0.38	0.52

Table 3: Performance of salient region detectors and descriptors on the OxFrei dataset.

5 Conclusion

References

- [Bay et al., 2008] Bay, H., Ess, A., Tuytelaars, T., and Van Gool, L. (2008). Speeded-up robust features (surf). *Comput. Vis. Image Underst.*, 110(3):346–359.
- [Dahl et al., 2011] Dahl, A. L., AanÅsø, H., and Pedersen, K. S. (2011). Finding the best feature detector-descriptor combination. In *3DIMPV*, pages 318–325. IEEE Computer Society.
- [Escalera et al., 2007] Escalera, S., Radeva, P., and Pujol, O. (2007). Complex salient regions for computer vision problems. In *CVPR*.
- [Flusser et al., 2009] Flusser, J., Suk, T., and Zitova, B. (2009). *Moments and Moment Invariants in Pattern Recognition*. Wiley.
- [Hassaballah et al., 2016] Hassaballah, M., Abdelmgeid, A. A., and Alshazly, H. A. (2016). Image Features Detection, Description and Matching. In Awad, A. and Hassaballah, M., editors, *IMAGE FEATURE DETECTORS AND DESCRIPTORS: FOUNDATIONS AND APPLICATIONS*, volume 630 of *Studies in Computational Intelligence*, pages 11–45. Springer.
- [Matas et al., 2002] Matas, J., Chum, O., Urban, M., and Pajdla, T. (2002). Robust Wide Baseline Stereo from Maximally Stable Extremal Regions. In *Proceedings BMVC*, pages 36.1–36.10.
- [Mikolajczyk et al., 2005] Mikolajczyk, K. et al. (2005). A comparison of affine region detectors. *International Journal of Computer Vision*, 65(1-2):43–72.
- [Mikolajczyk and Schmid, 2005] Mikolajczyk, K. and Schmid, C. (2005). A performance evaluation of local descriptors. *IEEE Trans. Pattern Anal. Mach. Intell.*, 27(10):1615–1630.
- [Ranguelova, 2016] Ranguelova, E. (2016). A Salient Region Detector for Structured Images. In *Proceedings of IEEE/ACS 13th Int. Conf. of Computer Systems and Applications (AICCSA)*, pages 1–8.
- [Snavely et al., 2008] Snavely, N., Seitz, S. M., and Szeliski, R. (2008). Modeling the world from internet photo collections. *Int. J. Comput. Vision*, 80(2):189–210.
- [Suk and Flusser, 2004] Suk, T. and Flusser, J. (2004). Graph method for generating affine moment invariants. In *17th International Conference on Pattern Recognition, ICPR 2004, Cambridge, UK, August 23-26, 2004.*, pages 192–195.

[Zagoruyko and Komodakis, 2015] Zagoruyko, S. and Komodakis, N. (2015). Learning to compare image patches via convolutional neural networks. *CoRR*, abs/1504.03641.